Philosophical Magazine
Publication details, including instructions for authors and subscription information:
http://www.tandfonline.com/loi/tphm20

Dislocation cross-slip mechanisms in aluminum

Congming Jin [a], Yang Xiang [b] & Gang Lu [c]

[a] Department of Mathematics, Zhejiang Sci-Tech University, Zhejiang, China

[b] Department of Mathematics, The Hong Kong University of Science and Technology, Clear Water Bay, Kowloon, Hong Kong

[c] Department of Physics and Astronomy, California State University Northridge, 18111 Nordhoff Street, Northridge, CA 91330-8268, USA

Available online: 15 Aug 2011

To cite this article: Congming Jin, Yang Xiang & Gang Lu (2011): Dislocation cross-slip mechanisms in aluminum, Philosophical Magazine, 91:32, 4109-4125

To link to this article: http://dx.doi.org/10.1080/14786435.2011.602030

Philosophical Magazine
Vol. 91, No. 32, 11 November 2011, 4109–4125

Dislocation cross-slip mechanisms in aluminum

Congming Jin[a], Yang Xiang[b]* and Gang Lu[c]

[a]*Department of Mathematics, Zhejiang Sci-Tech University, Zhejiang, China;* [b]*Department of Mathematics, The Hong Kong University of Science and Technology, Clear Water Bay, Kowloon, Hong Kong;* [c]*Department of Physics and Astronomy, California State University Northridge, 18111 Nordhoff Street, Northridge, CA 91330-8268, USA*

(*Received 5 February 2011; final version received 28 June 2011*)

We have systematically studied dislocation cross-slip in Al at zero temperature by atomistic simulations, focusing on the dependence of the transition paths and energy barriers on dislocation length and position. We find that for a short dislocation segment, the cross-slip follows the uniform Fleischer (FL) mechanism. For a longer dislocation segment, we have identified two different cross-slip mechanisms depending on the initial and final positions of the dislocation. If the initial and final positions are symmetric relative to the intersection of the primary and cross-slip planes, the dislocation cross-slips via the Friedel–Escaig (FE) mechanism. However, when the initial and final positions are asymmetric, the dislocation cross-slips via a combination of the FL and FE mechanisms. The leading partial folds over to the cross-slip plane first, forming a stair-rod dislocation at the intersection with which the trailing partial then merges via the FL mechanism. Afterwards, constrictions appear asymmetrically and move away from each other to complete the cross-slip via the FE mechanism.

Keywords: dislocation; cross-slip; aluminum; plastic deformation; transition path

1. Introduction

Cross-slip in f.c.c. crystals is a process by which a screw dislocation changes its slip plane from one {111} plane to another of the same type. Cross-slip plays an important role in the plastic deformation of metals and semiconductors, leading to hardening, pattern formation and dynamical recovery [1]. For example, cross-slip is responsible for the onset of stage III or dynamical recovery of the stress–strain relation; in dispersion-hardened materials, cross-slip leads to the lowering of the elastic energy of the glissile Orowan loops pinned by the particles [2]; cross-slip has also been recognized as a rate-controlling mechanism in creep deformation; in fatigue, cross-slip is responsible to the generation of persistent slip bands and other cell structures.

*Corresponding author. Email: maxiang@ust.hk

ISSN 1478–6435 print/ISSN 1478–6443 online

http://dx.doi.org/10.1080/14786435.2011.602030
http://www.tandfonline.com

Several models have been proposed for cross-slip in f.c.c. materials, including Schoeck–Seeger (SS) [3], Friedel–Escaig (FE) [4,5], and Fleischer (FL) models [6]. In the Schoeck–Seeger (SS) model [3], the two partials in a dissociated screw dislocation are recombined over some critical length before it re-dissociates in the cross-slip plane. The critical length has to be long enough for the combined screw segment to become unstable in the cross-slip plane where it bulges under the shear stress. The SS model requires a high activation energy, which is the sum of the recombination energy and the energy of two constrictions. According to the Friedel–Escaig (FE) model [4,5], cross-slip could occur more easily, taking advantage of existing constrictions along the screw dislocation. The constrictions act as nuclei for cross-slip; once they are formed, the constrictions move away from each other in the cross-slip plane where they dissociate into partials again to complete the cross-slip. The activation energy of the FE model is significantly lower than that of the SS model. The FE model has been semi-quantitatively confirmed by experiments for Cu [7,8]. The Fleischer (FL) model [6] differs from the two preceding models in suggesting that no complete constriction should be necessary for cross-slip. Instead, the stacking fault is assumed to fold over from the primary slip plane into the cross-slip plane continuously. In other words, the leading partial at the intersection of the two planes splits into a stair-rod dislocation at the intersection and a Shockley partial in the cross-slip plane, and then the trailing partial reacts with the stair-rod dislocation to form another Shockley partial in the cross-slip plane to complete the cross-slip process. The angle between the glide directions in the cross-slip and the primary planes could be either acute or obtuse, with the former having a lower activation energy; more importantly, both of them are energetically more favorable than the formation of a constriction over the same length. Although there are controversies about the energetic grounds of the Fleischer model [1,9,10], atomistic simulations [11,12] have suggested that a complete constriction of the stacking fault may not be necessary. However, the relative merits of these models and in particular, the conditions under which a certain model is operative are far from clear.

Two types of computational approaches, including continuum elasticity theory and atomistic simulations, have been used to explore cross-slip mechanisms. For example, Stroh estimated the cross-slip energy barrier via the FE mechanism using the line tension approximation of the two Shockley partial dislocations [13]. By approximating the shape of the screw dislocation with polygons, Duesbery has studied the three-dimensional cross-slip in the isotropic elastic limit [14]. Schoeck and Seeger, Wolf, and Schottky et al. have calculated the cross-slip energy barrier for f.c.c. metals using the Peierls–Nabarro model, assuming simple analytic forms for the dislocation shape [3,15,16]. Püschl and Schoeck have developed several elastic models to treat cross-slip and constrictions in various crystal structures and conditions [1,17–19]. Schoeck showed that the recombination energy of the two partials in the FE mechanism depends sensitively on the details of the γ-surface using the Peierls–Nabarro model, and determined necessary conditions on the applied stress for the onset of cross-slip [20]. On the other hand, the atomistic simulations have proven powerful in providing insights into the cross-slip mechanisms. For example, Rasmussen et al. have used the Nudged Elastic Band (NEB) [21] method in conjunction with the Embedded-Atom Method (EAM) to study cross-slip in Cu [22–24]. Rao et al. have employed a Green's function method coupled with

EAM to examine cross-slip in Ni [25]. These atomistic investigations found that the cross-slip processes in both Cu and Ni followed the FE mechanism.

In this paper, we systematically study dislocation cross-slip in Al using atomistic simulations. The study was motivated by the fact that Al has a much higher stacking fault energy than Cu and Ni, and thus the Shockley partials of the screw dislocation are very close to each other. Therefore, a complete constriction may not be necessary, i.e., the cross-slip may proceed via the FL mechanism. Indeed, early work based on the Peierls–Nabarro model for Al has revealed peculiar features of cross-slip that were at odds with the FE mechanism [26]. More recently, the FL mechanism has been observed computationally in Al nano-voids [27]. Furthermore, a constant strain rate molecular dynamics simulation for nano-crystalline Al has demonstrated that a significant number of dislocations at grain boundaries can cross-slip via the FL mechanism [28]. Since these investigations are concerned of nano-structures, it is not clear whether the same FL mechanism operates in coarse-grained bulk Al. Therefore, it is of great interest to obtain a complete understanding of the cross-slip mechanisms in Al, which is the aim of the research in this paper.

Dislocation cross-slip is a rare event requiring thermal activation and is usually beyond the capability of conventional molecular dynamics simulations. Although many methods have been proposed for simulations of rare events – each with its own merits and limitations – developing robust numerical methods for rare events is still an open and challenging research area. Many of these methods are based on transition state theory [29,30], such as the NEB method [21] and the string method [31–34]. These methods obtain the minimum energy path for the rare event at zero temperature, and the transition rate can be estimated from the energy barrier at the saddle point by an Arrhenius type formula [29,30]. Although these available transition state theory-based methods have been very successful in a wide range of applications, it is important to keep in mind that they depend on reasonably prescribed initial and final states as well as the initial guess of the minimum energy path. For dislocation cross-slip, since the screw dislocation core spreads over the primary plane, the cross-slip may not necessarily initialize from the center of the dislocation. Therefore it is important to examine how the cross-slip process depends on the initial and final positions of the dislocation, which has been overlooked in the existing simulation results obtained by transition state theory-based methods. In this paper, we employ the string method to determine the minimum energy path and energy barriers for the cross-slip in Al, taking into consideration the position dependence effect.

2. Cross-slip models of FE and FL

For convenience of the report of our simulations presented in Section 4, in this section, we summarize the classical FE and FL cross-slip models in a f.c.c. crystal.

A dislocation in f.c.c. materials is composed of two Shockley partials separated by a stacking fault. For example, in the (111) slip plane, the screw dislocation with

the Burgers vector $\mathbf{b} = \frac{a}{2}[1\bar{1}0]$ (a is the lattice constant) dissociates into two Shockley partials with the Burgers vectors $\mathbf{b}_1 = \frac{a}{6}[2\bar{1}\bar{1}]$ and $\mathbf{b}_2 = \frac{a}{6}[1\bar{2}1]$, respectively:

$$\frac{a}{2}[1\bar{1}0] = \frac{a}{6}[1\bar{2}1] + \frac{a}{6}[2\bar{1}\bar{1}]. \tag{1}$$

This screw dislocation can also lie in the $(\bar{1}\bar{1}1)$ plane and dissociate into two Shockley partials with the Burgers vectors $\mathbf{b}'_1 = \frac{a}{6}[1\bar{2}\bar{1}]$ and $\mathbf{b}'_2 = \frac{a}{6}[2\bar{1}1]$, respectively:

$$\frac{a}{2}[1\bar{1}0] = \frac{a}{6}[2\bar{1}1] + \frac{a}{6}[1\bar{2}\bar{1}]. \tag{2}$$

In the FE model [4,5], see Figure 1a, a pair of constrictions forms first along the screw dislocation, and they subsequently move away from each other in the cross-slip plane where they dissociate into partials again to complete the cross-slip.

In the FL model [6], the leading partial of the dissociated screw dislocation at the intersection of the primary and the cross-slip planes splits into a stair-rod dislocation at the intersection and a Shockley partial in the cross-slip plane, and then the trailing partial reacts with the stair-rod dislocation to form another Shockley partial in the cross-slip plane to complete the cross-slip process. If the glide direction in the cross-slip plane subtends an acute angle with the glide direction in the primary plane, see Figure 1b, the splitting reaction of the leading partial is given by

$$\frac{a}{6}[1\bar{2}1](\mathbf{b}_2) = \frac{a}{6}[2\bar{1}1](\mathbf{b}'_2) + \frac{a}{6}[\bar{1}\bar{1}0], \tag{3}$$

where $\mathbf{b}_2$ is the Burgers vector of the leading partial on the primary slip plane (111), $\mathbf{b}'_2$ is the Burgers vector of the resultant partial on the cross-slip plane $(\bar{1}\bar{1}1)$, and $\frac{a}{6}[\bar{1}\bar{1}0]$ is the Burgers vector of the stair-rod dislocation at the intersection. The stair-rod dislocation is a pure edge dislocation whose Burgers vector is neither on the primary or the cross-slip plane. Subsequently, the trailing partial with the Burgers vector $\mathbf{b}_1$ on the primary plane is attracted to the stair-rod dislocation and combines with it to give the second resultant partial with the Burgers vector $\mathbf{b}'_1$ on the cross-slip plane:

$$\frac{a}{6}[2\bar{1}\bar{1}](\mathbf{b}_1) + \frac{a}{6}[\bar{1}\bar{1}0] = \frac{a}{6}[1\bar{2}\bar{1}](\mathbf{b}'_1). \tag{4}$$

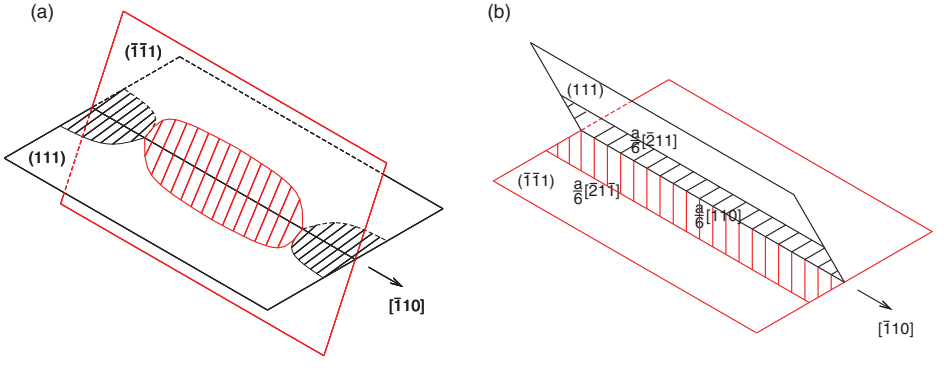

Figure 1. Models for cross-slip in f.c.c. crystals. (a) The FE model. (b) The FL model.

Similarly, if the glide in the cross-slip proceeds in a direction subtending an obtuse angle with the primary glide direction, the corresponding reactions are given by

$$\frac{a}{6}[1\bar{2}1](\mathbf{b}_2) = \frac{a}{6}[1\bar{2}\bar{1}](\mathbf{b}_1') + \frac{a}{3}[001], \tag{5}$$

$$\frac{a}{6}[2\bar{1}\bar{1}](\mathbf{b}_1') + \frac{a}{3}[001] = \frac{a}{6}[2\bar{1}1](\mathbf{b}_2'), \tag{6}$$

where the stair-rod dislocation has the Burgers vector of $\frac{a}{3}[001]$.

3. Computational method

We perform atomic simulations for Al at 0 K using the EAM potential developed by Mishin et al. [35], which gives excellent results including the stacking fault energy. It has been shown that the Shockley partial separation distance in the screw dislocation and the generalized stacking fault energy curve in Al obtained by the Mishin potential agree excellently with those from density function theory calculations ([36] and [37], respectively). The lattice constant a is 4.05Å with this potential, and the magnitude of the Burgers vector for a perfect dislocation is $b = \frac{\sqrt{2}}{2}a = 2.86$ Å. The three edges of the simulation cell are in the directions of $[\bar{1}10]$, $[\bar{1}\bar{1}2]$ and [112], respectively. The simulation cell contains $n_1 \times n_2 \times n_3$ atoms, where n_1, n_2, and n_3 are the number of atoms in each direction. The simulation cell is subject to periodic boundary conditions in the $[\bar{1}10]$ direction and free boundary conditions in the other two directions. We consider the cross-slip of a screw dislocation in Al with Burgers vector $b = \frac{a}{2}[1\bar{1}0]$. The $(1\bar{1}1)$ plane is designated as the primary slip plane of the screw dislocation and the $(\bar{1}\bar{1}1)$ plane as the cross-slip plane.

The crucial aspect of the present study is to determine the cross-slip mechanism and the activation energy barrier. To this end, the minimum energy transition path and the corresponding energy barrier are calculated using the string method [31–34]. The string method is an efficient transition-path-searching method and has been widely used in many applications such as the study of the energy landscape of ferromagnetic thin films [38], conformational changes of biomolecules [39,40], chemical reactions [41,42], and dislocation dynamics [34]. In the string method, a path on the energy landscape connecting the given initial and final stable states is represented by a continuous curve – the string. The minimum energy path is determined by evolving this curve under the potential force. Let q_1 and q_2 be two stable (initial and final) states of a system with a potential energy $V(q)$, where q represents a collection of relevant generalized coordinates uniquely specifying the state of the system. The minimum energy path between q_1 and q_2 is a curve φ in the configuration space connecting q_1 and q_2 that satisfies $(\nabla V)^{\perp}(\varphi) = 0$, where $(\nabla V)^{\perp}(\varphi) = \nabla V(\varphi) - (\nabla V(\varphi) \cdot \hat{\tau})\hat{\tau}$ is the component of ∇V normal to φ; $\hat{\tau}$ denotes the unit tangent of the curve φ. Physically, this equation means that for a minimum energy path, the generalized force normal to the curve vanishes. The solution of this equation is obtained by solving the following dynamics equation $\varphi_t = -\nabla V(\varphi)$ until convergence. Numerically, the curve φ is discretized into a series of images $\{\varphi(\alpha_i)\}$, $i = 0, 1, 2, \ldots, M$, where $\alpha \in [0, 1]$ is a parameter of the curve φ. In the present simulations, the gradient and the distance between any two states are calculated

in the $3N$-dimensional coordinate space, where N is the total number of atoms in the simulation cell. The evolution of the curve starts from an initial guess, and here we choose it to be the linear interpolation of the two stable states before and after the cross-slip. There are in total $M = 25$ images along the curve. The dynamics equation of the curve is solved using the forward Euler method combined with the upwind scheme for the discretisation of the gradient; the re-discretisation of the curve is implemented using a third-order polynomial interpolation scheme.

We have systematically examined the dislocation cross-slip mechanisms in Al, focusing on the effects of the length and the relative position of the dislocation before and after the cross-slip. In particular, as discussed in the Introduction, the possible position dependence of the cross-slip mechanisms has been overlooked in the existing atomistic simulations of the cross-slip mechanisms within the transition path framework. Here we examine this important issue by varying the relative position of the screw dislocation in the primary and cross-slip planes as illustrated in Figure 2. Without loss of generality, the center of the dislocation in the cross-slip plane is fixed at the position **0** as the final state of the cross-slip process. The possible initial positions of the dislocation in the primary plane are the nine nearby sites denoted by **0** to **8**. A particular cross-slip process is denoted by two numbers indicating the initial and final positions of the dislocation, respectively; e.g., in the **1-0** cross-slip, the dislocation is initially located at **1** in the primary plane and after the cross-slip, the dislocation is centered at **0** in the cross-slip plane. In the case of the **0-0** cross-slip, the two partials in both the primary and cross-slip planes are positioned *symmetrically* relative to the intersection of the two planes, whereas in the other cases, the partials are located *asymmetrically* with respect to the intersection.

Note that when a screw segment glides uniformly in its slip plane, its motion is subject to an energy barrier generated by the crystal lattice. This energy barrier

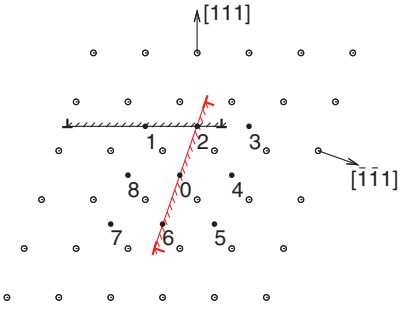

Figure 2. Possible positions of the screw dislocation in the (111) primary slip plane relative to that in the ($\bar{1}\bar{1}1$) cross-slip plane in the cross-slip process. The screw dislocation in the [$1\bar{1}0$] direction is pointing out of the paper, and the circles represent the atom positions in the ($\bar{1}10$) plane. The center of the screw dislocation in the cross-slip plane is fixed at the position **0** in the final state of the cross-slip process, and the possible positions of the center of the screw dislocation in the primary slip plane in the initial state are at positions **0-8**. As an example, the dislocation structures in the primary and cross-slip planes in the **1-0** cross-slip are shown schematically: the stacking fault before and after the cross-slip of the **1-0** cross-slip is shown by the shaded lines; the dislocation center is located at the mid-point of the shaded lines with the two partials at the two ends.

is proportional to the length of the dislocation segment and the energy barrier per unit length is referred to as the Peierls barrier. It is well-known that dislocations in f.c.c. crystals have low Peierls barriers, which provides a possible way for a screw dislocation segment in Al to change its position by uniform glide. However, for a long screw dislocation segment in Al (e.g., with a length of 36 atoms in our simulations), the total energy barrier for uniform glide is significantly higher than the thermal energy at room temperature (using the Peierls barrier 4.39×10^{-4} eV/Å of the screw dislocation in Al with the Mishin potential [37]), thus it is non-negligible in the study of the cross-slip process. This will be confirmed by the simulation results reported in Section 4 that the cross-slip mechanism is indeed position-dependent for a long screw segment.

4. Simulation results

For a perfect screw dislocation in Al, the two Shockley partials are very close to each other due to the high stacking fault energy. Using the Mishin EAM potential, we find that in Al the partial separation distance is $2.8b$. The partial distance is estimated as the distance over which the screw component of the relative displacement across the slip plane changes from $b/4$ to $3b/4$, following [43]. The magnitude of the edge component of the two partials is $0.14b$, much less than the hard-sphere model estimate of $\sqrt{3}b/6 = 0.29b$. In Figure 3, we show the obtained displacement densities of this screw dislocation. The displacement density is defined as the derivative of the relative displacement with respect to the atomic positions across the slip plane [43]. The positions of the partials are indicated by the two peaks of the density of the screw component in the primary plane, as shown in Figure 3a. Note that there are small screw and edge components in the cross-slip plane, as shown in Figure 3b, which agrees with the previous report in [26].

Note that the heavy overlap of the two Shockley partials of a screw dislocation in Al has been observed in simulations using empirical potentials [35], Peieris–Nabarro models [43–45], and density functional theory calculations [36]. This dissociation of a screw dislocation has many special properties compared with the typical Shockley

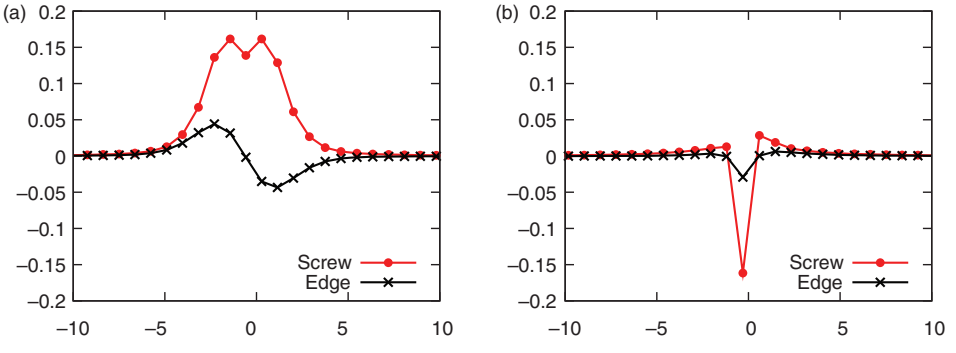

Figure 3. Displacement densities of a screw dislocation. (a) In the primary plane. (b) In the cross-slip plane. The horizontal axis is the atomic position given in b.

partial dissociation of dislocations in f.c.c. crystals, e.g., the much smaller magnitude of the edge components in partial dissociation in Al mentioned above. Currently in the literature, there is no well-accepted terminology for these types of partials, and various techniques have been used to identify these partials similar to the one used in this paper [35,36,45].

4.1. *A short dislocation segment*

In this subsection, we consider the cross-slip of a short screw dislocation. We choose the simulation cell with $6 \times 36 \times 36 = 7776$ atoms, and in particular, there are six atoms (17.2Å) along the dislocation line before the periodic boundary condition is applied. Increasing the numbers of atoms in the directions normal to the dislocation only leads to negligible changes in the results. We find that this short screw dislocation remains straight in the minimum energy path of the cross-slip process. The results may correspond to situations where a short dislocation segment is pinned by obstacles and cross-slips uniformly without bowing-out.

The cross-slip energy barrier and the minimum energy path for the **1-0** cross-slip are shown in Figures 4a and 5. In this case, the dislocation gliding direction in the primary plane and that in the cross-slip plane forms an acute angle, see Figure 2, and we find the cross-slip energy barrier as $0.028\,\mathrm{eV}/b$. This energy barrier is much smaller than that of Cu ($0.13\,\mathrm{eV}/b$) [22]. To probe the cross-slip mechanism, we examine the evolution of the displacement density of the dislocation in the primary and cross-slip planes along the minimum energy path. At the saddle point, a stair-rod dislocation is formed at the intersection. There is only *one* partial remaining in the primary plane as shown in Figure 5a. Note that this partial is the same left partial as in Figure 3 whose screw Burgers vector component is $b/2$. At the same time, a new partial with $b/2$ in its screw component is formed in the cross-slip plane shown in Figure 5b. Both partials are of the Shockley type as indicated by their edge and screw components. The results suggest that the cross-slip essentially follows the FL model uniformly over the dislocation length: the leading partial folds over to the cross-slip and leaves behind a trailing partial in the primary plane. As a result, a stair-rod dislocation is formed at the intersection.

The results for the **0-0** cross-slip are summarized in Figure 6 in the differential displacement plots. The differential displacement is defined as the relative screw displacement between neighboring atoms connected by an arrow whose length is proportional to the magnitude of the displacement [46]. It is observed that the screw dislocation first shifts to the left in the primary plane, then cross-slips following the FL mechanism as shown previously for the **1-0** cross-slip, and finally the dislocation shifts upward in the cross-slip plane. The corresponding energy barrier is $0.028\,\mathrm{eV}/b$ shown in Figure 4b, the same as that of the **1-0** cross-slip. The energy barriers for the shifts of a short dislocation segment are small owing to the low Peierls barriers of dislocations in Al.

We have also studied dislocation cross-slip from other possible initial positions and the results are summarized in the following. The **5-0** cross-slip is similar to the **1-0** cross-slip. For **3-0** and **7-0** where the primary and the cross-slip planes form an obtuse angle, the dislocation cross-slips follow the FL model, the same as **1-0** with

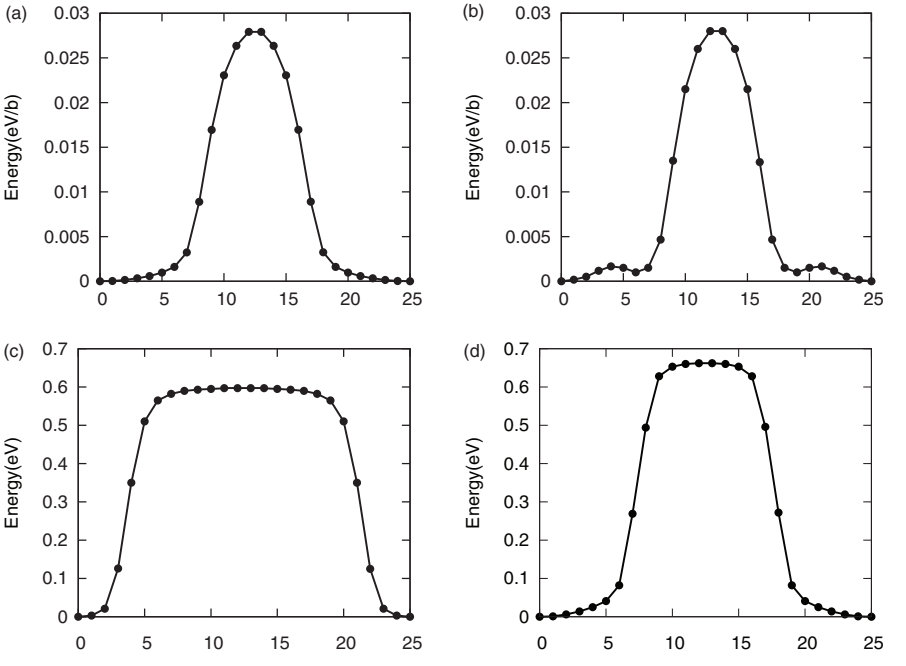

Figure 4. Energy variation along the cross-slip minimum energy path. The numbers on the horizontal axis are the indices of the image states along the minimum energy path, with 0 being the initial state and 25 being the final state. (a) Short dislocation segment, **1-0** cross-slip. (b) Short dislocation segment, **0-0** cross-slip. (c) Long dislocation segment, **0-0** cross-slip. (d) Long dislocation segment, **1-0** cross-slip.

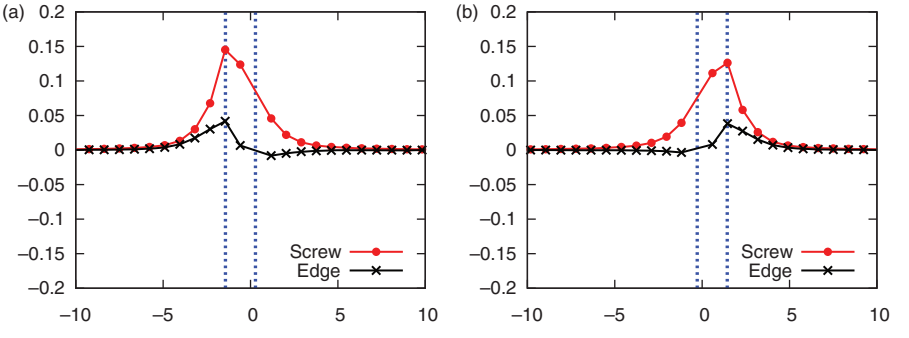

Figure 5. The displacement density at the saddle point of the minimum energy path for the **1-0** cross-slip of the short dislocation segment: (a) at the primary plane; (b) at the cross-slip plane. The vertical dashed lines indicate the original (in (a)) or final (in (b)) positions of the partials, and the horizontal axis is the atomic position in units of *b*.

necessary shifts in the two planes. For example, the **3-0** cross-slip can be completed by a shift from position **3** to position **1**, followed by the **1-0** cross-slip; alternatively, it can also be completed by the **1-0** cross-slip upward and then a shift down to position **0** in the cross-slip plane. In the cases of **2-0** and **6-0**, the dislocation first shifts in the

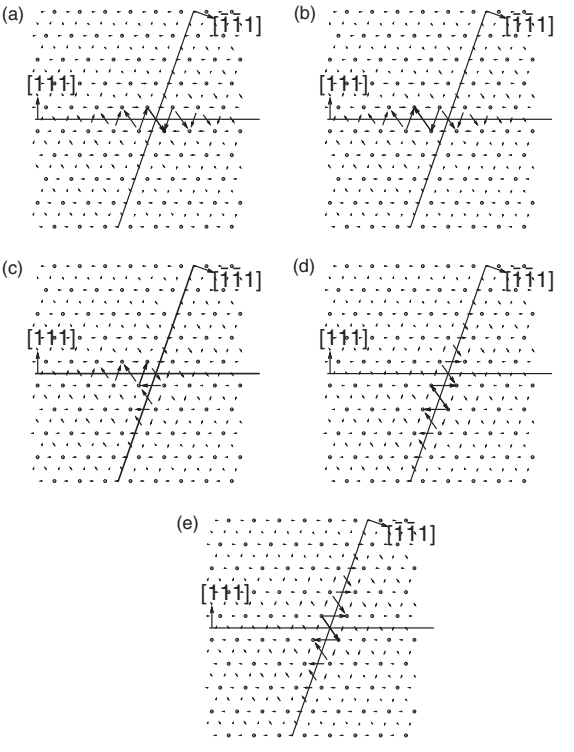

Figure 6. The differential displacement plots for the **0-0** cross-slip of the short dislocation segment: (a) the initial state, (b) the stable state after a shift in the primary plane, (c) the saddle point state, (d) the stable state after the cross-slip, and (e) the final state after a shift in the cross-slip plane from (d). The circles represent the positions of atoms. The arrows indicate the direction and the amplitude (normalized by $b/2$) of the relative displacement between the connected atoms.

primary plane and then cross-slips following the FL mechanism as the **1-0** or **5-0** cross-slip. In the cases of **4-0** and **8-0**, the dislocation first cross-slips following the FL mechanism as the **1-0** or **5-0** cross-slip and then shifts in the cross-slip plane.

To conclude, for the short segment cross-slip, there is only one distinctive cross-slip process, characterized by the **1-0** cross-slip which follows the FL model uniformly. The energy barrier is $0.028\,\mathrm{eV}/b$, much smaller than that of $0.13\,\mathrm{eV}/b$ in Cu via the uniform FE mechanism [22]. Our results are consistent with the observations that the FL mechanism is operative in Al nano-structures where the length of the dislocation is small [27,28].

4.2. *A long dislocation segment*

Next, we turn to a long screw dislocation segment. We choose the simulation cell with $36 \times 36 \times 36 = 46{,}656$ atoms, and in particular, there are 36 atoms along the dislocation. Increasing the number of atoms in the directions normal to the

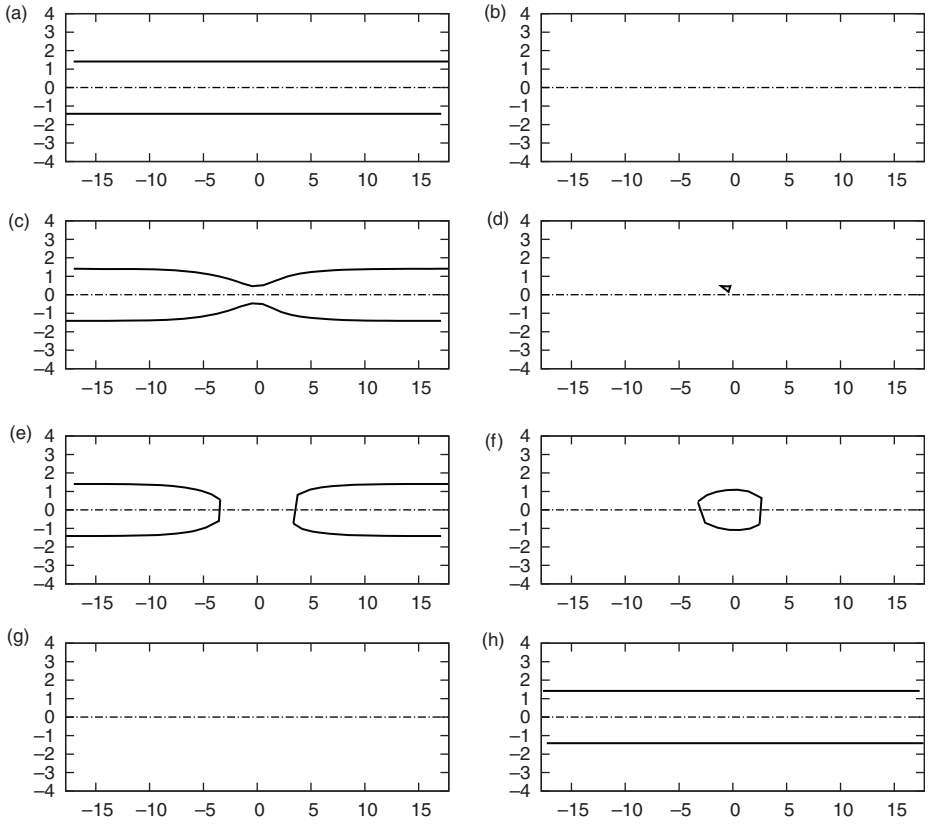

Figure 7. The positions of the partials in the primary and the cross-slip planes along the minimum energy path for the **0-0** cross-slip of the long dislocation segment. The partials are initially along the horizontal axis in the primary plane. The horizontal dashed line represents the intersection of the two slip planes. The length is given in units of b. The left panel (a), (c), (e), and (g) shows the evolution of the partial dislocation positions in the primary plane. The right panel (b), (d), (f), and (h) shows the same in the cross-slip plane.

dislocation only gives negligible changes in the results. We find that the partials of this long screw dislocation are able to bow out during the cross-slip process.

The process of the **0-0** cross-slip is summarized in Figure 7. The two partials in the primary plane are positioned *symmetrically* relative to the intersection of the primary and cross-slip planes. They bow to each other at some point and merge symmetrically relative to the intersection. As soon as the constriction starts to form, the cross-slip proceeds symmetrically as shown in Figure 8. Both the screw and edge components of the dislocation transfer simultaneously and gradually from the primary plane to the cross-slip plane in a symmetric manner. Figure 8 shows the intermediate stage of this process where half of the dislocation including both the screw and edge components has been transferred from the primary plane to the cross-slip plane. It is instructive to note the difference between Figure 8 and Figure 5. There are *two* partials at each plane in Figure 8 whereas there was only *one* partial

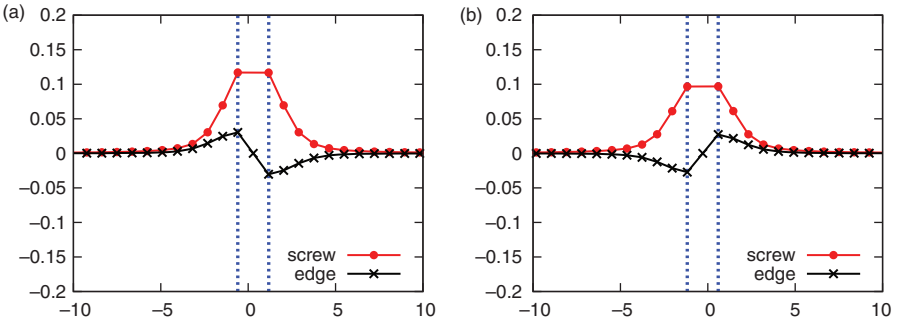

Figure 8. Displacement density at the recombination of the partials of the long dislocation segment in (a) the primary plane, and (b) the cross-slip plane. The horizontal axis is the atomic position given in units of b. The positions of the partials are indicated by the dashed lines.

at each plane in Figure 5. As shown in Figure 7, the cross-slip is completed as the the constrictions move away from each other. Therefore the *symmetric* **0-0** cross-slip follows the FE mechanism. The energy barrier of the cross-slip, which is also the energy of the constriction pair, is 0.60 eV, shown in Figure 4c.[1]

On the other hand, the **1-0** cross-slip proceeds asymmetrically or off-center owing to the asymmetric initial and final positions relative to the intersection. As shown in Figure 9, one of the partials in the primary plane is located *closer* to the intersection (hence termed the leading partial) than the other partial (termed the trailing partial). The two partials bow to each other *asymmetrically*, shown in Figure 9c, and the leading partial folds over to the cross-slip plane and simultaneously grows in the cross-slip plane, resulting in a stair-rod dislocation at the intersection. The formation of the stair-rod dislocation is identical to that in the cross-section of the short segment and is reminiscent of the FL mechanism, see Figure 5. It is important to note that the cross-slip is not initiated from a constriction as in the FE mechanism, but rather from the direct transfer or the fold-over of the leading partial. When the trailing partial reaches the intersection and merges with the stair-rod dislocation, the constrictions start to form at the intersection; the constrictions subsequently move away from each other to complete the cross-slip process, following the FE mechanism. Therefore the **1-0** cross-slip is characterized by a combination of the FL and FE mechanisms in a two-step process – it starts with the FL mechanism and is completed by the FE mechanism. The energy barrier for the cross-slip is 0.66 eV (see Figure 4d), which is also the energy of the asymmetric constriction pair. The energy of this asymmetric cross-slip is slightly higher than that of the symmetric **0-0** cross-slip. We should clarify that by "asymmetric", we mean that the constrictions appear off-center normal to the dislocation (the vertical direction in Figure 9). It does not refer to the fact that the two constrictions are distinctive and have different energies [22,23,25].

It is important to note the difference between the observed mechanism and the original FL mechanism [6,47]; the observed **1-0** cross-slip does not follow the FL mechanism all the way to the end. Instead, as discussed above, part of the dislocation cross-slips by the FL mechanism first, with the two asymmetric constrictions formed

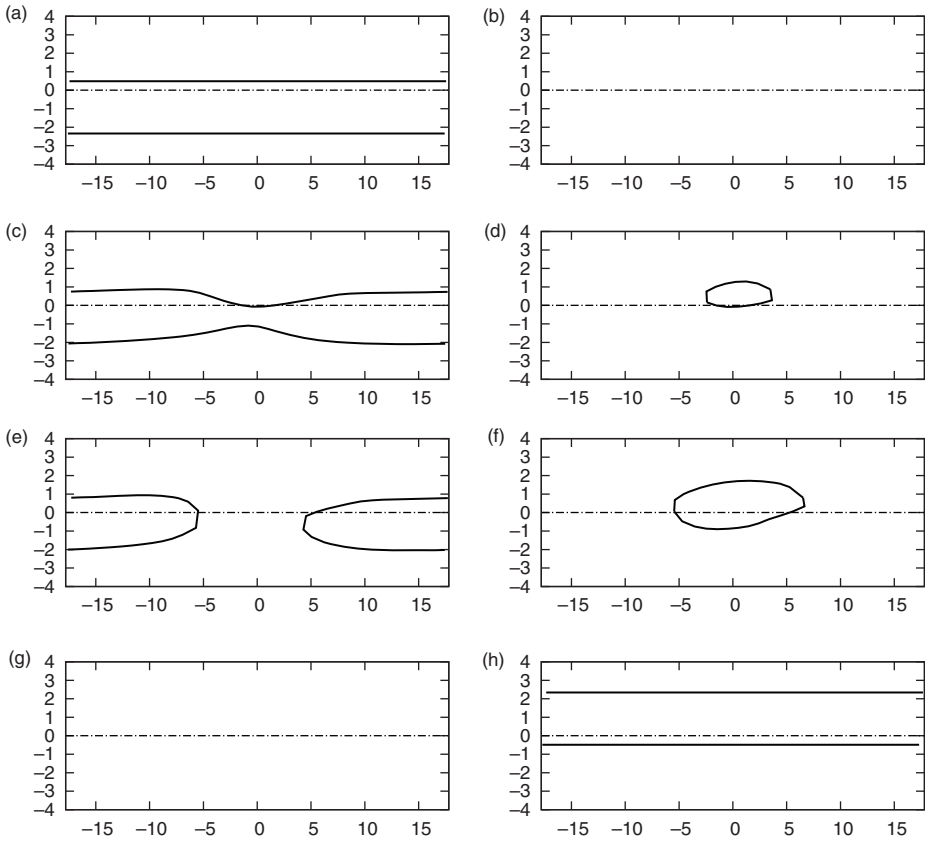

Figure 9. The positions of the partials in the primary and the cross-slip planes along the **1-0** cross-slip minimum energy path for the long screw dislocation segment. The dislocation is initially along the horizontal axis in the primary plane. The horizontal dashed line represents the intersection of the two planes. The length is given in units of *b*. The left panel (a), (c), (e), and (g) shows the evolution of the partial dislocation positions in the primary plane. The right panel (b), (d), (f), and (h) shows the same in the cross-slip plane.

as shown in Figure 9e and f, and the remaining part of the dislocation cross-slips by the FE mechanism. This cross-slip mechanism has only a slightly higher energy (0.66 eV) than that of the FE mechanism (0.60 eV), therefore it could be operative under certain stress conditions and/or geometric restrictions. Further research is needed to identify such conditions. This combination of FL and FE mechanisms with an asymmetric constriction pair has never been reported in the past to our knowledge.

To further understand the difference between the symmetric and the asymmetric constrictions, we plot the energy of each cross-sectional plane perpendicular to the dislocation line in Figure 10 at the saddle point in Figure 4c or d. The energy is defined with respect to the initial straight dislocation before cross-slip. The sum of the energy over all atomic planes (the area under the curve) gives the total energy of the constriction pair or the energy barrier for the cross-slip as shown in Figure 4c or d.

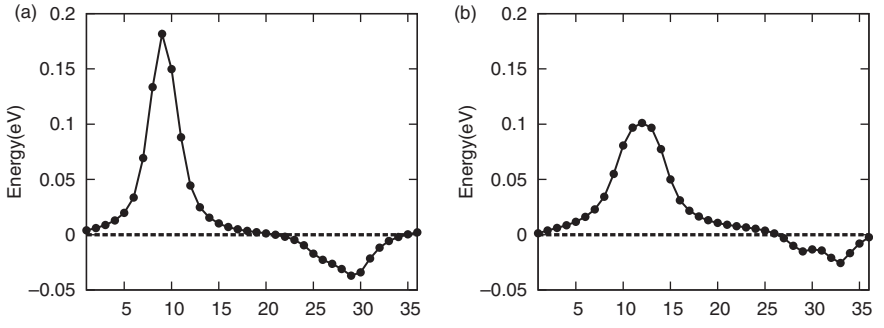

Figure 10. The energy in each cross-sectional plane perpendicular to the dislocation at the saddle point of the cross-slip of a long dislocation segment in Figure 4c or d. (a) Symmetric constriction pair for the **0-0** cross-slip. (b) Asymmetric constriction pair for the **1-0** cross-slip. The unit on the horizontal axis is b.

We find that for both the symmetric and the asymmetric constriction pairs, one constriction in the pair is energetically favorable and the other is unfavorable. This result is similar to what has been observed in the literature for Cu and Ni [22,23,25]. However, the symmetric constriction pair has a sharper energy profile than the asymmetric case although the total energy difference between them is small, about 10%.

We summarize the results for other possible cross-slips for the long dislocation segment. In the case of **8-0**, the dislocation first shifts to position **0** and then follows the same cross-slip process as in **0-0**. For **7-0** where the primary and the cross-slip planes form an obtuse angle, the dislocation cross-slips the same as **0-0** but with a shift in the primary plane before the cross-slip and a shift in the cross-slip plane afterwards. The other cases behave in the same way as those mentioned above owing to symmetry. There are two distinctive cross-slip processes – **0-0** symmetric and **1-0** asymmetric. All other cross-slips adapt one of the two processes. The energetically most favorable cross-slip process is the one observed in the **0-0** case, whose energy barrier is 0.60 eV. Comparing with the cross-slip energy barrier of 0.028 eV/b for the short dislocation segment, we conclude that there is a critical dislocation length, $\sim 22b$, above which the dislocation cross-slips following the mechanisms observed for the long segment; otherwise, it cross-slips uniformly via the FL mechanism.

It is difficult to extract quantitative information of cross-slip from deformation experiments. Experimentally, an activation barrier of 1.15 ± 0.37 eV [8] has been inferred in a temperature range 250–410 K for Cu, while such an estimate does not exist for Al [1]. It is expected, however, that the activation energy barrier for Al should be lower than that of Cu owing to the smaller partial separation distance in Al.

5. Conclusions and discussion

We have systematically examined the dislocation cross-slip process in Al at zero temperature, focusing on the cross-slip dependence on dislocation length and position. We find that for the short dislocation segment ($< 22b$), the cross-slip

proceeds with the Fleischer (FL) mechanism, independent of the dislocation position. This result is consistent with the observation that the cross-slip in Al nano-structures follows the FL mechanism. On the other hand, for the longer dislocation segment ($>22b$), we have identified two different cross-slip mechanisms depending on the initial and final positions of the dislocation relative to the intersection – symmetric or asymmetric. In both cases, the cross-slip is completed by the motion of two constrictions following essentially the Friedel–Escaig (FE) model. However, they differ in the manner by which the constrictions are formed. For the symmetric **0-0** cross-slip, the two partials merge symmetrically at the intersection and form the symmetric constrictions. For the asymmetric **1-0** cross-slip, the leading partial reaches the intersection first and folds over to the cross-slip plane, forming a stair-rod dislocation at the intersection. The trailing partial merges with the stair-rod dislocation and then the constrictions appear asymmetrically. This asymmetric, two-step cross-slip mechanism has never been reported before. The minimal cross-slip energy barriers for the short and the long dislocation segments are 0.028 eV/b via the FL mechanism and 0.60 eV via the FE mechanism, respectively.

Although the new mechanism we have found – the asymmetric **1-0** cross-slip mechanism–does not have the lowest energy barrier, its barrier 0.66 eV is only slightly higher than the minimal barrier via FE mechanism. Thus this mechanism could be operative under certain conditions such as applied stress and/or geometric restrictions, or the presence of free surfaces. This will be explored in future work.

Finally, we have overcome the limitations of the current transition state theory-based minimum energy path-finding methods [21,31–34] by systematic examination of the position dependence in the cross-slip process. The finite temperature string method [48,49] will be employed in future work to further confirm the results by generating multiple paths for the initial guess in the minimum energy path search. The entropy effect in the cross-slip process will also be explored in future work (W. E, W. Ren and E. Vanden-Eijnden, unpublished results and [34]).

Acknowledgements

The work of CJ is supported by the National Science Foundation of China under Grant No. 11001244 and the Science Foundation of Zhejiang Sci-Tech University (ZSTU) under Grant No. 0713680-Y. The work of YX is partially supported by Hong Kong RGC Direct Allocation Grant DAG_S09/10.SC04. The work at the California State University Northridge was supported by DOE and ONR.

Note

1. The decrease of the energy profiles at later stages in Figure 4c and d for long dislocation segments is due to the periodic boundary conditions of the simulation cell.

References

[1] W. Püschl, Prog. Mater. Sci. 47 (2002) p.415.
[2] L.M. Brown and R.K. Ham, *Dislocation-particle interactions*, in *Strengthening Methods in Crystals*, A. Kelly and R.B. Nicholson, eds., Applied Science, London, 1971, p.9.

[3] G. Schoeck and A. Seeger, *Activation energy problems associated with extended dislocations, Report of the Conference on Defects in Crystalline Solids*, The Physical Society, London, 1955, p.340.
[4] J. Friedel, *Regarding Seeger's paper on work hardening*, in *Dislocations and Mechanical Properties of Crystals*, J.C. Fisher, W.G. Johnston, T. Thomson and T. Vreeland Jr, eds., John Wiley, New York, 1957, p.330.
[5] B. Escaig, *Cross-slipping process in the f.c.c. structure*, in *Proceedings of the Battelle Colloquium in Dislocation Dynamics*, A.R. Rosenfield, G.T. Hahn, A.L. Bement Jr and R.I. Jaffee, eds., McGraw-Hill, New York, 1968, p.655.
[6] R.L. Fleischer, Acta Metall. 7 (1959) p.134.
[7] J. Bonneville and B. Escaig, Acta Metall. 27 (1979) p.1477.
[8] J. Bonneville, B. Escaig and J.L. Martin, Acta Metall. 36 (1988) p.1989.
[9] A.J.E. Foreman, Acta Metall. 3 (1955) p.322.
[10] A.N. Stroh, Phil. Mag. 3 (1958) p.625.
[11] T.A. Parthasarathy and D.M. Dimiduk, Acta Mater. 44 (1996) p.2237.
[12] M.S. Duesbery, Model. Simul. Mater. Sci. Eng. 6 (1998) p.35.
[13] A.N. Stroh, Proc. Phys. Soc. B 67 (1954) p.427.
[14] M.S. Duesbery, N.P. Louat and K. Sadananda, Acta Metall. Mater. 40 (1992) p.149.
[15] H. Wolf, Z. Naturforschg. 15a (1960) p.180.
[16] G. Schottky, A. Seeger and V. Speidel, Phys. Stat. Sol. 9 (1965) p.231.
[17] W. Püschl, Phys. Stat. Sol. (b) 162 (1990) p.363.
[18] W. Püschl and G. Schoeck, Mater. Sci. Eng. A 164 (1993) p.286.
[19] W. Püschl and G. Schoeck, *Dissociation and constriction energies in extended dislocations*, in *Proceedings of the 10th ICSMA*, H. Oikawa, H. Maruyama, S. Takeuchi and M. Yamaguchi, eds., The Japan Institute of Metals, Sendai, Japan, 1994, p.97.
[20] G. Schoeck, Phil. Mag. Lett. 89 (2009) p.505.
[21] H. Jónsson, G. Mill and K.W. Jacobsen, *Nudged elastic band method for finding minimum energy paths of transitions*, in *Classical and Quantum Dynamics in Condensed Phase Simulations*, B.J. Berne, G. Ciccoti and D.F. Coker, eds., World Scientific, Singapore, 1998, p.385.
[22] T. Rasmussen, K.W. Jacobsen, T. Leffers, O.B. Pedersen, S.G. Srinivasan and H. Jónsson, Phys. Rev. Lett. 79 (1997) p.3676.
[23] T. Rasmussen, K.W. Jacobsen, T. Leffers and O.B. Pedersen, Phys. Rev. B 56 (1997) p.2977.
[24] T. Vegge, T. Rasmussen, T. Leffers, O.B. Pedersen and K.W. Jacobsen, Phys. Rev. Lett. 85 (2000) p.3866.
[25] S. Rao, T.A. Parthasarathy and C. Woodward, Phil. Mag. A 79 (1999) p.1167.
[26] G. Lu, V.V. Bulatov and N. Kioussis, Phys. Rev. B 66 (2002) p.144103.
[27] J. Marian, J. Knap and M. Ortiz, Acta Mater. 53 (2005) p.2893.
[28] E. Bitzek, C. Brandl, P.M. Derlet and H. Van Swygenhoven, Phys. Rev. Lett. 100 (2008) p.235501.
[29] S. Glasstone, K.J. Laidler and H. Eyring, *The Theory of Rate Processes*, McGraw-Hill, New York, 1941.
[30] G.H. Vineyard, J. Phys. Chem. Solids. 3 (1957) p.121.
[31] W. E, W. Ren and E. Vanden-Eijnden, Phys. Rev. B 66 (2002) p.52301.
[32] W. E, W. Ren and E. Vanden-Eijnden, J. Chem. Phys. 126 (2007) p.164103.
[33] C. Jin, Commun. Comput. Phys. 2 (2007) p.1220.
[34] C. Jin, W. Ren and Y. Xiang, Scripta Mater. 62 (2010) p.206.
[35] Y. Mishin, D. Farkas, M.J. Mehl and D.A. Papaconstantopoulos, Phys. Rev. B 59 (1999) p.3393.

[36] C. Woodward, D.R. Trinkle, L.G. Hector Jr and D.L. Olmsted, Phys. Rev. Lett. 100 (2008) p.045507.
[37] T. Tsuru, Y. Kaji and Y. Shibutani, J. Comput. Sci. Technol. 4 (2010) p.185.
[38] W. E, W. Ren and E. Vanden-Eijnden, J. Appl. Phys. 93 (2003) p.2275.
[39] W. Ren, E. Vanden-Eijnden, P. Maragakis and W. E, J. Chem. Phys. 123 (2005) p.134109.
[40] T.F. Miller III, E. Vanden-Eijnden and D. Chandler, Proc. Natl. Acad. Sci. USA, 104 (2007), p.14559.
[41] Y. Kanai, A. Tilocca, A. Selloni and R. Car, J. Chem. Phys. 121 (2004) p.3359.
[42] M. Yoon, S. Han, G. Kim, S.B. Lee, S. Berber, E. Osawa, J. Ihm, M. Terrones, F. Banhart, J.C. Charlier, N. Grobert, H. Terrones, P.M. Ajayan and D. Tománek, Phys. Rev. Lett. 92 (2004) p.075504.
[43] G. Lu, N. Kioussis, V.V. Bulatov and E. Kaxiras, Phys. Rev. B 62 (2000) p.3099.
[44] G. Schoeck, Mater. Sci. Eng. A 333 (2002) p.390.
[45] Y. Xiang, H. Wei, P.B. Ming and W. E, Acta Mater. 56 (2008) p.1447.
[46] V. Vitek, R.C. Perrin and D.K. Bowen, Phil. Mag. 21 (1970) p.1049.
[47] J.P. Hirth and J. Lothe, *Theory of Dislocations*, 2nd ed., John Wiley, New York, 1982.
[48] W. E, W. Ren and E. Vanden-Eijnden, J. Phys. Chem. B 109 (2005) p.6688.
[49] W. Ren, E. Vanden-Eijnden, P. Maragakis and W. E, J. Chem. Phys. 123 (2005) p.134109.